Yerbilimleri, 2021, 42 (3), 287-300, 794158
Hacettepe Üniversitesi Yerbilimleri Uygulama ve Araştırma Merkezi Bülteni (*Bulletin of the Earth Sciences Application and Research Centre of Hacettepe University*

YERBİLİMLERİ
Bulletin for Earth Sciences

ISSN: 2687- 2978

Spatial and temporal analysis of seismicity of the Pütürge Fault, and Gutenberg-Richter parameters before and after Sivrice-Doğanyol earthquake (Mw6.8) of January 24, 2020

24 Ocak 2020 Sivrice-Doğanyol depremi (Mw6.8) öncesi ve sonrası Pütürge Fayı'nın depremselliğinin ve Gutenberg-Richter parametrelerinin mekânsal ve zamansal analizi

HALUK EYİDOĞAN [1*]

[1]Saksılı Sokak, Deniz Apt., 3/1, D.2, Heybeliada, Adalar, 34970, İstanbul, Turkey.

Geliş *(received)*: 12 Eylül (*September*) 2020 Kabul *(accepted)*: 21 Eylül (*September*) 2021

ABSTRACT

The seismological characteristics of earthquake activity before and after January 24, 2020 (Mw6.8) Sivrice-Doğanyol earthquake were studied for the period between January 1, 2018 and August 6, 2020. Spatial and temporal distributions of epicenters of this activity, focal mechanism solutions and Gutenberg-Richter parameters (Mc, a- and b-values) show remarkable patterns. Mechanism solutions of Mw≥5.0 magnitude earthquakes prove that the Pütürge Fault is a left-lateral strike-slip fault with a northwest dipping plane. It was observed that the increase in Mc value before January 24, 2020 Sivrice-Doğanyol mainshock started simultaneously with a light earthquake of Mw4.9 on December 27, 2019, 28 days before the main earthquake. The decrease trend in b-value started on September 8, 2019, 139 days before the mainshock, and on December 27, 2019, the b-value decreased to the lowest level of 0.6. The reason for the increase in Mc value and the significant decrease of the b-value before the January 24, 2020 Sivrice-Doğanyol earthquake may be the effect of the increase in the effective stress on the Pütürge Fault before the earthquake and the change in physical process. Similar findings regarding the decrease of the b-value of seismic activity before large and strong earthquakes have been observed and published for many earthquakes in the world. Studies on this subject are ongoing, and b-value can be considered to use as a long or mid-term warning mechanism before a major earthquake in the future.

Keywords: Seismicity of Pütürge Fault, Gutenberg-Richter equation, completeness magnitude, decrease in b-value, earthquake forecasting

ÖZ

24 Ocak 2020 (Mw6.8) Sivrice-Doğanyol depremi öncesi ve sonrası deprem aktivitesinin sismolojik özellikleri 1 Ocak 2018-6 Ağustos 2020 tarihleri arasında incelenmiştir. Bu aktivitenin dış merkez konumlarının mekânsal ve zamansal dağılımları, fay mekanizması çözümleri ve Gutenberg-Richter parametreleri (Mc, a- ve b-değerleri) dikkate değer örüntüler göstermiştir. Mw≥5.0 büyüklüğündeki depremlerin mekanizma çözümleri, Pütürge Fayı'nın kuzeybatıya eğimli ve sol yanal doğrultu atımlı bir fay olduğunu kanıtlamaktadır. 24 Ocak 2020 öncesi Mc değerindeki artışın, ana depremden 28 gün önce, 27 Aralık 2019'da Mw4.9'luk hafif bir sarsıntıyla eş zamanlı başladığı gözlenmiştir. b-değerindeki düşüş eğilimi, 8 Eylül 2019'da ana şoktan 139 gün önce başlamış ve 27 Aralık 2019'da 0.6 değeri ile en düşük seviyeye gerilemiştir. 24 Ocak 2020 Sivrice-Doğanyol depreminden önce Mc değerindeki artışın ve b-değerinin önemli ölçüde azalmasının nedeni, deprem öncesi Pütürge Fayı üzerindeki aktif gerilmenin artması ve fiziksel özelliklerin depremden önceki değişimi ile ilgili olabilir.

https://doi.org/10.17824/yerbilimleri.794158

*Sorumlu Yazar/ Corresponding Author: *eyidogan@itu.edu.tr*

Sismik aktiviteye ait b-değerinin büyük ve kuvvetli depremler öncesi azalmasına dair benzer bulgular, dünyadaki birçok deprem için gözlenmiş ve yayınlanmıştır. Bu konudaki çalışmalar sürmekte olup, b-değerinin gelecekte büyük deprem öncesi bir tahmin mekanizması gibi kullanılması düşünülebilir.

Anahtar Kelimeler: *Pütürge Fayı'nın depremselliği, Gutenberg-Richter bağıntısı, tamlık büyüklüğü, b-değerinde düşüş, depremi önceden tahmin*

INTRODUCTION

Physical changes in active faults and the state of stress conditions before strong or large earthquakes are important research topics for seismologists. A wide variety of studies, ranging from rock breaking experiments in the laboratory to sophisticated investigation of earthquakes recorded in the field, provide an increase in knowledge of physical changes before and after earthquakes (Utsu, 1971; Main et al., 1989; Helmstetter et al., 2003; Schorlemmer et al., 2005; Scholz, 2015; Riviere et al., 2018; Wu et al., 2018; Gulia and Wiemer, 2019; Nanjo, 2019). The Gutenberg-Richter (G-R) empirical equation (Gutenberg and Richter, 1944) has an important role in understanding the seismicity characteristics of a region and tectonics-earthquake relationships. Mathematically, G-R equation represents the relationship between each unit of magnitude greater than the magnitude Mc (completeness magnitude) of the earthquake sequence occurring in a region and the cumulative number of occurrences of an earthquake of that magnitude (Gutenberg and Richter 1944; Mogi, 1962). Spatial and temporal changes of a- and b-value parameters representing the G-R equation given as Log_{10} N(M)=a-bM are associated with many geological, tectonics, geophysical and seismological elements. The a-value is an indicator of the earthquake activity degree of the earthquake zone and factors such as the observation range and the number of earthquakes affect this value. It can be said that the b-value, which is the slope of the function in the G-R equation, represents the characteristics of the stress changes developed in the earth's crust. Based on the findings of independent earthquake studies, b-value is described as "strain meter" (Wu et al., 2018). It has been observed that the b-value is remarkably affected by the changes in the physical parameters in the ground such as the stress variation around the faults and fractures in the ground, the temperature change in the volcanic and geothermal source areas, the pore pressure changes of the fluid in the rocks and the fault/fracture density.

Given the interrelationships of these physical changes with each other, investigation of the b-value makes a significant contribution to determining the physical processes that activate earthquakes. The average b-value for the world is accepted as approximately 1.0, but it has been observed that it varies between 0.3-2.0 in seismotectonic areas with different characteristics (Utsu, 1971).

It is essential to calculate the completeness of earthquake magnitudes with the least error in order to obtain the correct a- and b-values. In the process of calculating the G-R equation, it is recommended to homogenize the earthquake magnitudes in the study area. Weaknesses in the determination of the Mc value may lead to an increase in the error of a- and b-values, and thus deficiencies in the evaluation of the earthquake characteristics of the area under investigation (Hainzl, 2016). It is recommended that the completeness ratio be 90% and above over the whole area and observation time. The smaller the magnitude of the Mc represents the earthquakes, the higher the number of earthquake stations and recording performance in that area is considered. Although the earthquake station performance is good, if significant changes in Mc value are observed, this may be a finding indicating high and calm periods of seismicity (Popandopoulos et al., 2016). The spatial and temporal changes of Mc, a- and b-values have been the subject of many studies, including understanding the properties of tectonic activity and faults with earthquakes, as well as forecasting earthquakes (Riviere et al., 2018; Brodsky, 2019).

In this article, the seismological characteristics of the earthquake activity between January 1, 2018 and August 6, 2020 on the 97 km long Pütürge Fault of the Eastern Anatolian Fault extending between Sivrice-Pütürge (Duman and Emre, 2013, Emre et al. 2016) were examined. For this purpose, the spatial and temporal variations of the epicentral distributions, focal mechanism solutions and variables Mc, a- and b-values of the G-R equation of earthquakes on the Pütürge Fault were evaluated.

SEISMOTECTONICS OF EAST ANATOLIAN FAULT

The Anatolian Plate (Ketin, 1969; McKenzie, 1978) which was compressed due to the N-S movement of the African, Arabian and Eurasian Plates, formed a very complex seismotectonic structure. Anatolian Plate exhibits a "tectonic escape" movement towards the west at an average speed of 20 mm per year (Şengör, 1987).A significant amount of the westward escape movement of the plate occurs over the North Anatolian Fault and the East Anatolian Fault.

The southern branch of the East Anatolian Fault extending between Karlıova and Kırıkhan was discovered by Allen (1969), mapped by Arpat and Şaroğlu (1972) and later studied by many earth scientists (Duman and Emre, 2013; McKenzie 1978, Arpat and Şaroğlu, 1975; McKenzie, 1976; Jackson and McKenzie, 1984; Dewey et al., 1986; Westaway and Arger, 1996; Taymaz et al., 1991; Aktuğ et al., 2016). The East Anatolian Fault, 580 kilometers long, performs an average of one-third and two-thirds of the westward movement of the Anatolian Plate (25-35 millimeters/year) (Duman and Emre, 2013; Taymaz et al., 1991).

The East Anatolian Fault consists of many interconnected fault segments (Table 1, Figure 1). According to the historical and instrumental records, many strong and destructive earthquakes occurred on the East Anatolian Fault (Duman and Emre, 2013; Ambraseys, 1989; Ambraseys and Jackson, 1998). According to the current catalogs, earthquakes near the Pütürge Fault are as follows: 3 May 1874 Ms7.1 and 3 March 1875 Ms6.7 earthquakes in the north of Sivrice Lake, 499 Ms7.0, 1104 Ms6.5 and 4 December 1905 Ms6.8 earthquakes between Çelikhan and Pütürge. It is controversial whether the earthquake of December 4, 1905, at the northeast end of the Erkenek Fault, loaded a significant stress accumulation despite being adjacent to the Pütürge Fault (Taymaz et al., 1991). After exhibiting a long seismic inactivity in terms of strong earthquakes (Duman and Emre, 2013), the Pütürge Fault ended the seismic quiescent period with the Mw6.8 magnitude earthquake on January 24, 2020 and created many aftershocks.

Table 1. Seismotectonic properties of fault segments of the northern branch of the East Anatolian Fault that extends between Karlıova-Kırıkhan. * Code: The fault codes (Emre et al., 2016). LL: Left-lateral strike-slip fault. **Melgar et al. (2020).

*Çizelge 1. Doğu Anadolu Fayı'nın Karlıova-Kırıkhan arasında uzanan kuzey kolunun fay segmentlerinin sismotektonik özellikleri. * Kod: Fay kodları (Emre et al., 2016). LL: Sol yanal doğrultu atımlı fay. ** Melgar et al., (2020).*

Fault Segment	Type	Code*	Fault Length (km)	Slip (mm/year) (min-max)	Depth (km)	Magnitude (Observed)	Magnitude (Estimated)
Karlıova Fault	LL	2-1	31	8-8	18-20	--	6.8
Ilıca Fault	LL	2-2	37	8-8	18-20	6.8 (M_s)	--
Palu Fault	LL	2-3	77	9-10	18-20	--	7.1
Gökdere Jog	LL	2-3-1	14	9-10	18-18	--	6.4
Gökdere Jog	LL	2-3-2	24	9-10	18-18	--	6.7
Gökdere Jog	LL	2-3-3	24	9-10	18-18	--	6.7
Pütürge Fault	LL	2-4	97	--	20**	6.8 (M_w)	7.4
Erkenek Fault	LL	2-5	77	6-7	18-20	--	7.3
Pazarcık Fault	LL	2-6	82	6-7	18-20	--	7.3
Amanos Fault	LL	2-7	114	4-5	--	--	7.5

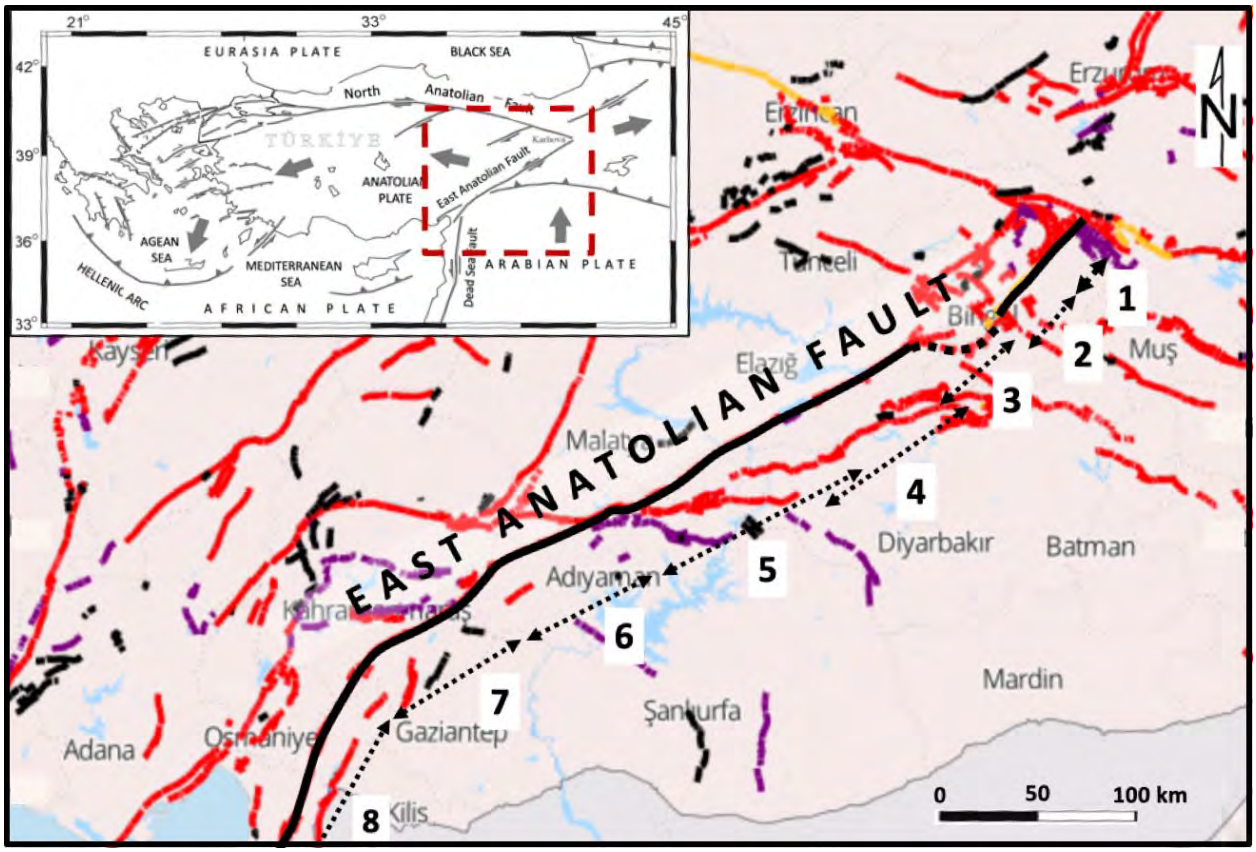


Figure 1. Locations of fault segments of the East Anatolian Fault (thick black line) extending between Karlıova and Kırıkhan (Duman and Emre, 2013). 1- Karlıova Fault, 2- Ilıca Fault, 3- Gökdere Jog, 4- Palu Fault, 5- Pütürge Fault, 6- Erkenek Fault, 7- Pazarcık Fault, 8- Amanos Fault.

Şekil 1. Doğu Anadolu Fayı'nın (kalın siyah çizgi) Karlıova ile Kırıkhan arasında uzanan fay segmentlerinin konumları (Duman ve Emre, 2013). 1- Karlıova Fayı, 2- Ilıca Fayı, 3- Gökdere Jogu, 4- Palu Fayı, 5- Pütürge Fayı, 6- Erkenek Fayı, 7- Pazarcık Fayı, 8- Amanos Fayı.

DATA ANALYSIS AND THE SEISMICITY OF PÜTÜRGE FAULT

Homogenization of earthquake magnitude

5,482 earthquakes with a magnitude of M≥1.0 were selected from the AFAD earthquake database (AFAD, 2020a) in the area bounded by latitudes 38.10° N-38.65° N and longitudes 38.50° E- 39.60° E between January 1, 2018 and August 6, 2020. The reason for processing the data two years before the 24 January 2020 earthquake is to recognize the background seismicity properties of the Pütürge Fault before the Mw6.8 magnitude mainshock and to evaluate these data together with the mainshock and aftershocks properties.

The magnitude scales of the majority of the earthquakes selected from the AFAD catalogue (AFAD, 2020a) are reported in local magnitude ML, but those with M≥4.0 are given as moment magnitude Mw. Considering that this difference may cause deviations in the calculation of the parameters targeted by our research, it was decided to convert the earthquake magnitudes into the Mw scale, which is widely used today. For this purpose, a literature search was conducted to convert earthquakes with different magnitude scales to Mw. Studies on this subject have been examined (Grünthal et al., 2009; Goertz-Allmann et al., 2011; Dost et al., 2018; Bora, 2016) and Goertz-Allmann et al. (2011)'s equations (1), (2) and (3), and for duration magnitudes Md Bora (2016)'s equation (4) were used.

$$Mw = 0.594ML + 0.985\ (ML < 2) \quad (1)$$

$$Mw = 1.327 + 0.253ML + 0.085ML^2 (2 \leq ML \leq 4) \quad (2)$$

$$Mw = ML - 0.3\ (ML > 4) \quad (3)$$

$$Mw = 0.93Md + 0.35 \quad (4)$$

Recent seismicity of Pütürge Fault (2018-2020)

The histograms of the number of earthquakes occurring around Sivrice-Pütürge between January 1, 2018 and August 6, 2020, depending on the epicenter depths and homogenized magnitudes (Figure 2a, b) show that the majority of the earthquakes are shallow and their magnitudes vary between 1.6≤Mw≤2.0. Although the reported earthquake depths generally seem appropriate to the seismotectonic character of the region, hypocenter depths of almost 85% of the earthquakes we analyzed accumulate at 7 km (Figure 2b). This is because the number and distribution of earthquake stations are insufficient for small earthquakes and the earthquake seismic velocity structure is not well known. Due to this inadequacy, especially the depth values of small earthquakes cannot be determined sensitively by conventional algorithms and thus they are fixed to a depth value of 7 km by the operators at AFAD Seismological Research Department (AFAD, 2020a).

In the period before the January 24, 2020 (Mw6.8) earthquake, three activities including earthquakes of magnitude Mw≥4.0 were observed. These events occurred on January 19, 2018 (Mw4.1), April 4, 2019 (Mw5.2) and December 27, 2019 (Mw4.9), respectively (Figure 3a, c). The January 19, 2018 earthquake occurred in the north of Pütürge, the April 4, 2019 and December 27, 2019 earthquakes were in the north (7 km) of the epicenter of the January 24, 2020 (Mw6.8) earthquake (Figure 3a, b). The 27 December 2019 (Mw4.9) earthquake, which occurred 28 days before the main earthquake of January 24, 2020 (Mw6.8), gives the impression of a precursor earthquake, but is another subject of research.

The January 24, 2020 mainshock produced numerous aftershocks, covering an area of 60 km long and 25 km wide along the Pütürge Fault and locating along the fault on both sides of the epicenter (Figure 3b, Eyidogan and Hobbs, 2020). According to the data reported by AFAD (2020a), earthquake epicenters show two main clusters, located in the east and west of the Euphrates River of the Pütürge Fault (Figure 3b). Similar phenomenon is also evident during the earthquake activity period before the January 24, 2020 mainshock (Figure 3a). Interestingly, the aftershock activity gradually decreased in the area where the Pütürge Fault crossed the Euphrates River, namely between longitudes 38.9° E and 39.1° E and the Pütürge Fault produced less aftershocks in this area. After June 2020, we see that the aftershock activity has become much more active in terms of both number and strong earthquakes. In other words, the aftershocks migrated to the southwest over time (Figure 4).

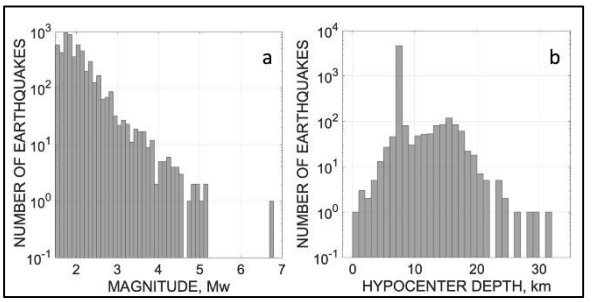


Figure 2. Histograms of a) earthquake magnitude and b) hypocenter depth of 5.482 earthquakes with magnitudes 1.6≤Mw≤6.8 on the Pütürge Fault between January 1, 2018 and August 6, 2020. The vertical axes of the graphs are shown in logarithmic scale to make the earthquake numbers more visible. The depths of most of the hypocenters are reported as 7 km.

Şekil 2. 1 Ocak 2018 ile 6 Ağustos 2020 tarihleri arasında Pütürge Fayı üzerinde 1.6≤Mw≤6.8 büyüklüğünde 5.482 depremin a) deprem büyüklüğü ve b) deprem iç merkez derinliği histogramları. Deprem sayılarını daha görünür kılmak için grafiklerin dikey eksenleri logaritmik olarak gösterilmiştir. Deprem iç merkezlerinin çoğunun derinliği 7 km olarak rapor edilmiştir.

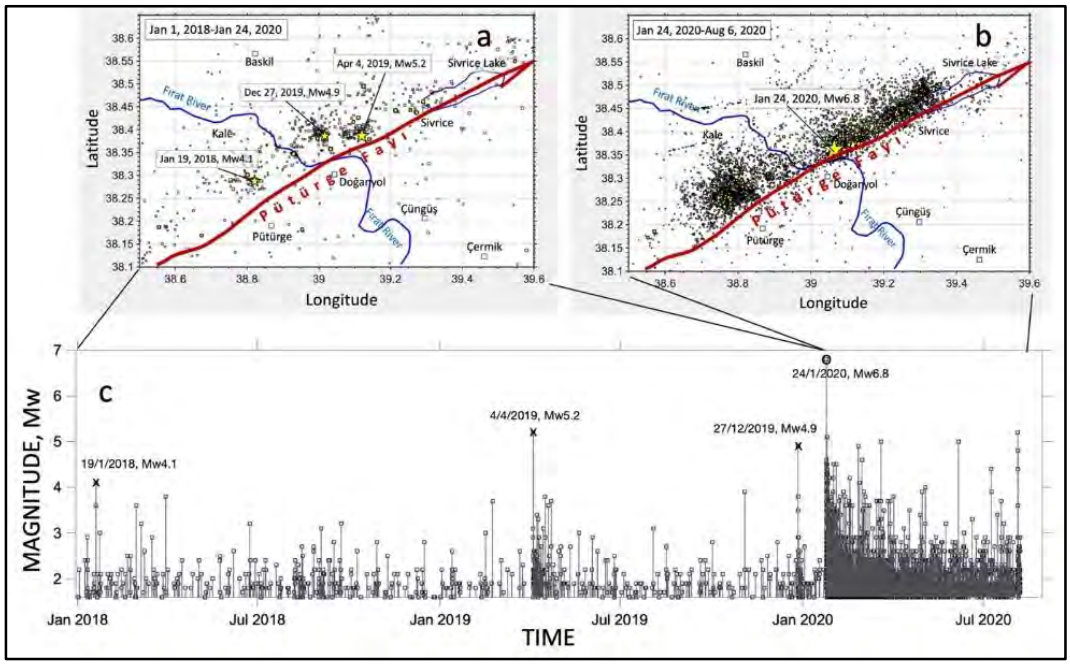


Figure 3. Spatial and temporal distribution of the homogenized Mw magnitude of the earthquake activity around the Pütürge Fault between January 1, 2018 and August 6, 2020. Magnitudes range from 1.6≤Mw≤6.8. (a) Earthquake activity before the Mw6.8 mainshock between January 1, 2018 and January 24, 2020, (b) earthquake activity between January 24, 2020-August 6, 2020, (c) earthquake activity between January 1, 2018 and August 6, 2020.
Şekil 3. 1 Ocak 2018 ile 6 Ağustos 2020 arasındaki Pütürge Fayı çevresindeki deprem aktivitesinin homojenleştirilmiş Mw büyüklüğü değerlerinin mekânsal ve zamansal dağılımı. Büyüklükler 1.6≤Mw≤6.8 arasında değişmektedir. (a) 1 Ocak 2018 ile 24 Ocak 2020 arasındaki Mw6.8 ana şoku öncesi deprem aktivitesi, (b) 24 Ocak 2020-6 Ağustos 2020 arasındaki deprem aktivitesi, (c) 1 Ocak 2018 ile 6 Ağustos 2020 arasındaki deprem aktivitesi.

In order to understand the seismotectonic properties of the Pütürge Fault, the focal mechanism solutions (Table 2) of Mw≥5.0 earthquakes reported by AFAD (2020a, b) for the period January 1, 2018-August 6, 2020 are shown on the seismicity map (Figure 5). Five of the six solutions belong to the earthquake activity that started on January 24, 2020, and these solutions confirm the direction of the Pütürge Fault and the left-lateral strike-slip fault movement. Melgar et al. (2020) using HR-GNSS (Hiper Global Navigation Satellite System) found that the rupture on the Pütürge Fault during the mainshock started from the northeast and progressed to the southwest. According to the authors, a significant part of the slip occurred at a depth of 2 to 10 km during the earthquake. According to GNSS data, a left lateral displacement (slip) of 20-30 cm occurred on the Pütürge Fault during the earthquake (Melgar et al., 2020). Kurcer et al. (2020) conducted geological and paleo-seismological studies in the field and observed that surface deformations developed during the earthquake in the approximately 48 km long section between Hazar Lake and Pütürge Town.

According to InSAR data, approximately 30 cm left lateral slip occurred on the Pütürge Fault. The focal mechanism solution of the 4 April 2019 (Mw5.2) earthquake, which is at a point close to the mainshock of January 24, 2020 (Mw6.8), represents the left-lateral strike-slip movement of the Pütürge Fault (Table 2, Figure 1). The northwest dipping left lateral strike-slip fault planes (Table 2) obtained in the mechanism solutions of the Mw6.8 main shock earthquake and the Mw5.1 aftershock earthquake explain why the epicenters of the earthquakes are located in the northwest of the fault. According to the analyzes made by USGS, the fault associated with the Mw6.8 magnitude earthquake has an azimuth of 246 °. The largest displacement of the rupture along the fault is 2.0 meters and it is 20 km southwest from the center of the earthquake. Studies conducted with different observations reveal that the Pütürge Fault is in the azimuth direction of 244 ° -246 ° and the aftershocks cluster in the northwest of the fault due to the fact that the fault is slightly inclined towards the northwest.

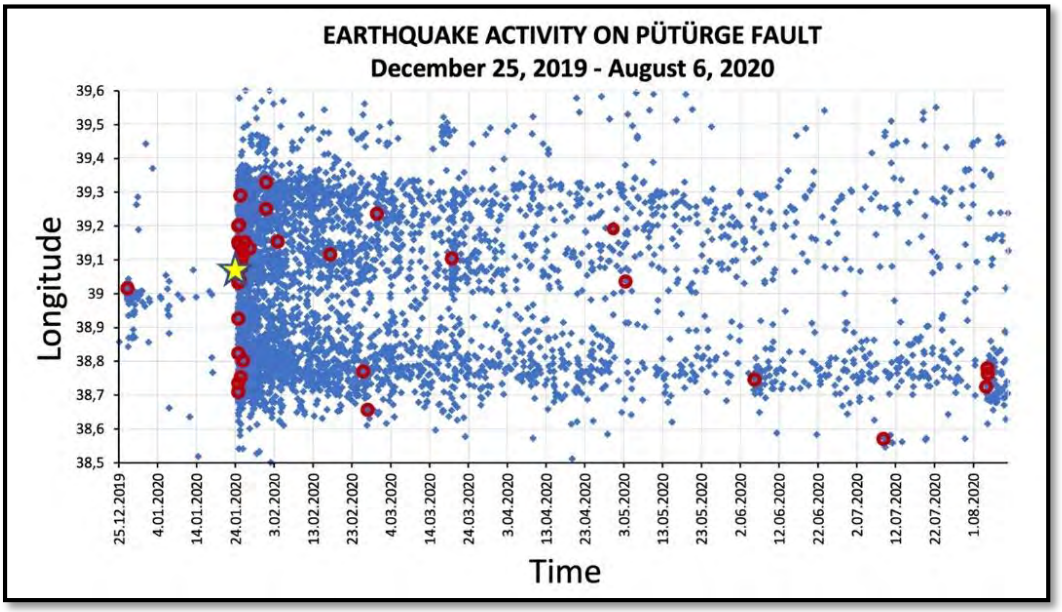


Figure 4. Earthquake activity of the Pütürge Fault between December 25, 2019 and August 6, 2020. There was a light earthquake of 4.9 magnitude on 27 December 2020, 28 days before the 24 January 2020 (Mw6.8) earthquake. After February 2020, a seismically quiescent region was formed in the aftershock distribution between the northeast and southwest part of the Pütürge Fault (longitudes between 38.85° E- 39.00° E). Yellow star indicates the mainshock (Mw6.8). Earthquake activity increased in number and magnitude in the southwestern part Pütürge Fault after June 2020. Red circles indicate the earthquakes with magnitude Mw≥4.0.

Şekil 4. Pütürge Fayı'nın 25 Aralık 2019 ile 6 Ağustos 2020 arasındaki deprem aktivitesi. 24 Ocak 2020 (Mw6.8) depreminden 28 gün önce, 27 Aralık 2020'de 4.9 büyüklüğünde hafif bir deprem olmuştur. Şubat 2020'den sonra Pütürge Fayı'nın kuzeydoğu ve güneybatı kesimi arasındaki artçı sarsıntı dağılımında (38.85°D- 39.00°D boylamları arasında) sismik olarak sakin bir alan gelişmiştir. Sarı yıldız ana depremi (Mw6.8) gösterir. Deprem aktivitesi, Pütürge Fayı'nın güneybatı kesiminde Haziran 2020'den sonra sayı ve büyüklük olarak artmıştır. Kırmızı daireler Mw≥4.0 büyüklüğündeki depremleri göstermektedir.

Table 2. Focal mechanism solutions of earthquakes with magnitudes Mw≥5.0 on the Pütürge Fault between January 1, 2018 and August 6, 2020. SA: Direction of fault, DA: Dip of the fault, RA: Slip angle of the fault. FMS: Focal mechanism solution, MT: Moment tensor solution. FM: First motion solution (AFAD, 2020a,b).

Çizelge 2. 1 Ocak 2018 ile 6 Ağustos 2020 tarihleri arasında Pütürge Fayı üzerindeki Mw≥5.0 büyüklüğündeki depremlerin odak mekanizması çözümleri. SA: Fayın yönü, DA: Fayın eğimi, RA: Fayın kayma açısı. FMS: Odak mekanizması çözümü türü, MT: Moment tensör çözümü, FM: İlk hareket çözümü (AFAD, 2020a, b).

Date-Origin Time	Latitude	Longitude	Mw	SA°	DA°	RA°	Type	FMS
04/04/2019 17:31:07	38.3865	39.1205	5.2	76.0	83.0	6.0	MT	
24/01/2020 17:55:11	38.3593	39.0630	6.8	248.0	76.0	1.0	MT	
25/01/2020 16:30:07	38.3740	39.1310	5.1	244.0	58.0	-7.0	MT	
19/03/2020 17:53:31	38.3720	39.1041	5.0	75.0	82.0	-6.0	FM	
05/06/2020 18:06:20	38.2576	38.7455	5.0	244.0	14.0	-10.0	MT	
04/08/2020 09:37:34	38.2193	38.7243	5.2	60.0	79.0	6.0	MT	

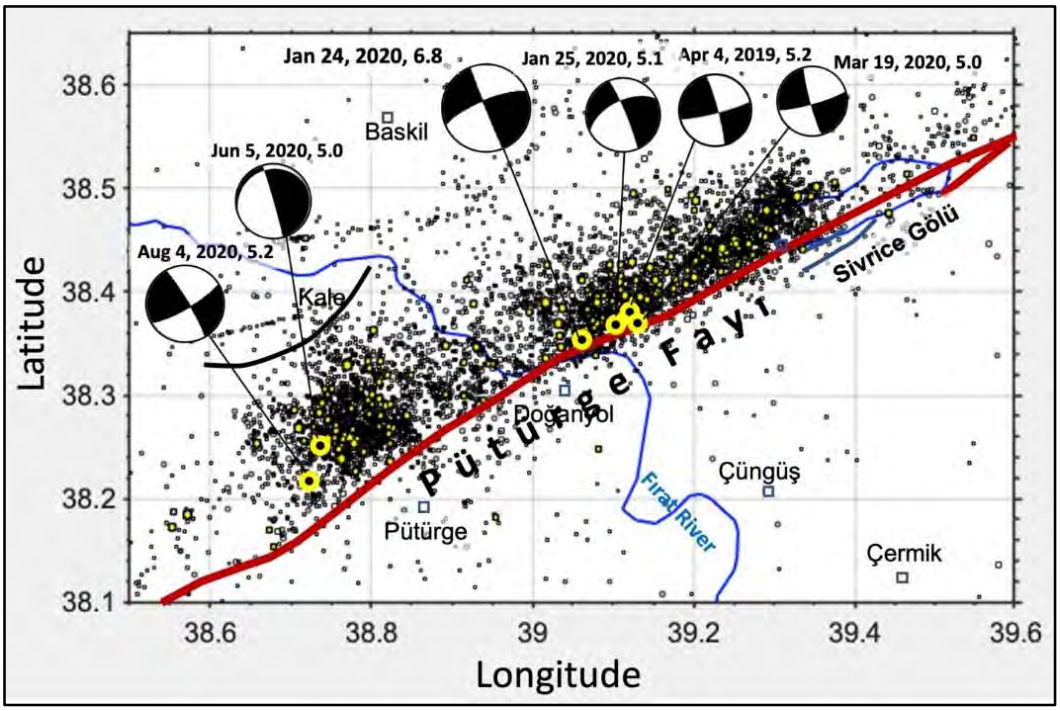


Figure 5. Epicenters of the earthquake activity with magnitudes Mw≥1.6 on the Pütürge Fault between January 1, 2018 and August 6, 2020. Fault Focal mechanism solutions are given for earthquakes with magnitude Mw≥5.0 (Yellow colored circles, Table 2). Mechanism solutions are taken from AFAD (2020a, b).

Şekil 5. 1 Ocak 2018 ile 6 Ağustos 2020 arasındaki Pütürge Fayı üzerinde Mw≥1.6 büyüklüğünde deprem aktivitesinin dış Merkez dağılımları. Mw≥5.0 büyüklüğündeki depremler için fay odak mekanizması çözümleri verilmiştir (Sarı renkli daireler, Çizelge 2). Mekanizma çözümleri AFAD'dan (2020a, b) alınmıştır.

ANALYSIS OF GUTENBERG-RICHTER (G-R) PARAMETERS OF THE EARTHQUAKE ACTIVITY OF 1 JANUARY 2018-6 AUGUST 2020

After the steps of obtaining earthquake data, homogenization of earthquake magnitudes and evaluation of earthquake focal mechanism solutions, G-R parameters were calculated and their spatial and temporal changes were evaluated. Determination of Mc, a and b-values of homogenized earthquakes and evaluation of their spatial and temporal changes were made with ZMAP7, the new version of ZMAP software developed by Wiemer (2001) and operated under MATLAB R2018b (MATLAB, 2020).

Determination of Mc, a- and b-values

The Mc value of the earthquake activity between January 1, 2020 and August 6, 2020 was calculated by the maximum curvature method (Wiemer and Wyss, 2002). The maximum likelihood method (Aki, 1965; Shi and Bolt, 1982) was used to obtain the b-value more sensitively. Based on the calculated optimum Mc value, a- and b-values were determined by minimizing errors. Thus, the G-R equation that best represents the earthquake activity on the Pütürge Fault between January 1, 2018 and August 6, 2020 was calculated as $Log10\ N(Mw) = 5.531 - 1.04Mw$ for a 0.1 magnitude step (Figure 6). During the determination of the b-value, the deviation from linearity performance and bootstrapping uncertainty control shows a negligible change in the a-value of 0.2% and the b-value with a negligible change by 1.0%.

Spatial distribution of G-R variables

Various values have been tested for grid intervals, sizes of the space window that will move at each grid point and the minimum number of earthquakes in each window area in the calculation of Mc and b-value. Thus, the criteria representing the least standard deviation were determined. For Sivrice-Doğanyol earthquake activity, the grid spacing was 0.7 km, the minimum number of earthquakes falling within the window was 50, the radius at each grid point was 7.0 km, and the closest event number for the variable window was 150.

The spatial distribution of the values obtained for Mc, a-value, b-value and standard deviation of b-value is shown in Figure 7. In areas where earthquakes are intense, Mc varies between 2.0-2.1 (Figure 7a). It was observed that the b-value ranged between 0.8-1.3 (Figure 7b) and the a-value between 4.0-5.0 (Figure 7c). The standard deviation of the b-value fell below the value of 0.05 in areas where earthquakes are concentrated (Figure 7d). The reason for the increase of b-value and standard deviation at the boundaries of the study area may be due to the insufficient number of earthquakes. Similarly, in areas where earthquake activity is reduced, the a-value decreases. It can be suggested that the lowest standard deviations of the b-value in the places where earthquakes are most intense are related to the completeness of the Mc value and the increase in the number of earthquakes per unit area. When the spatial distribution of the b-value is examined, it is observed that the Mc and b-value increase where the Pütürge Fault crosses the Euphrates River. As can be noticed from the epicentral distributions, we see that this phenomenon accompanies two separate earthquake cluster patterns in the northeast and southwest of the Pütürge Fault (Figure 4, Figure 5).

Temporal distribution of Mc and b-value

Graphs were prepared and evaluated for temporal changes of Mc and b-values before and after the mainshock of January 24, 2020 (Mw6.8) (Figure 8). Temporal changes of the Mc and b-value were obtained for at least 50 earthquakes and 300 sample window sizes. Mc values of the earthquake activity on the Pütürge Fault remained fairly stable from November 6, 2018 to December 25, 2019 and varied in the 1.8-1.9 band. However, before the mainshock on January 24, 2020, the Mc value started to increase after the Mw4.9 earthquake on December 27, 2019 i.e. 28 days ago. Mc value rapidly decreased to 1.8 after the mainshock of January 24, 2020 (Figure 8a).

Between November 6, 2018 and September 8, 2019, the b-value of the earthquake activity changed between 1.1-1.3 and started to decline on September 8, 2019 (Figure 8b). The b-value reached the lowest value of 0.6 on 27 December 2020, and started to increase again after staying at this value for a short time (Figure 8b). December 27, 2020 is also the date when a Mw4.9 magnitude earthquake occurred close to the location of the mainshock. Shortly after this date, when the b-value reached 0.8, on January 24, 2020 Mw6.8 Sivrice-Doğanyol earthquake occurred. When the temporal changes of Mc and b-values are evaluated together, the anomalies that occur with the decrease of the b-value to 0.6 value between September 8, 2019 and December 27, 2019 and the rapid increase of the Mc value after December 27, 2020 can be associated with the stress change process that led to the mainshock.

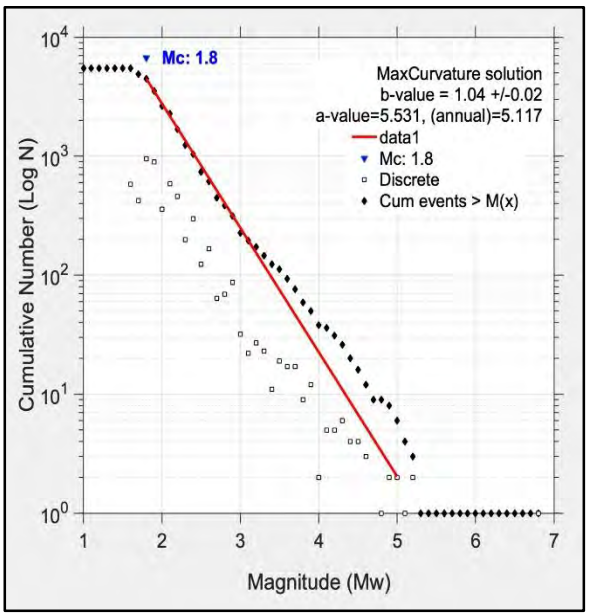


Figure 6. G-R graphs of 5.482 earthquakes on the Pütürge Fault between January 1, 2018 and August 6, 2020.

Şekil 6. 1 Ocak 2018 ile 6 Ağustos 2020 arasında Pütürge Fayı'nda meydana gelen 5.482 depremin G-R grafiği.

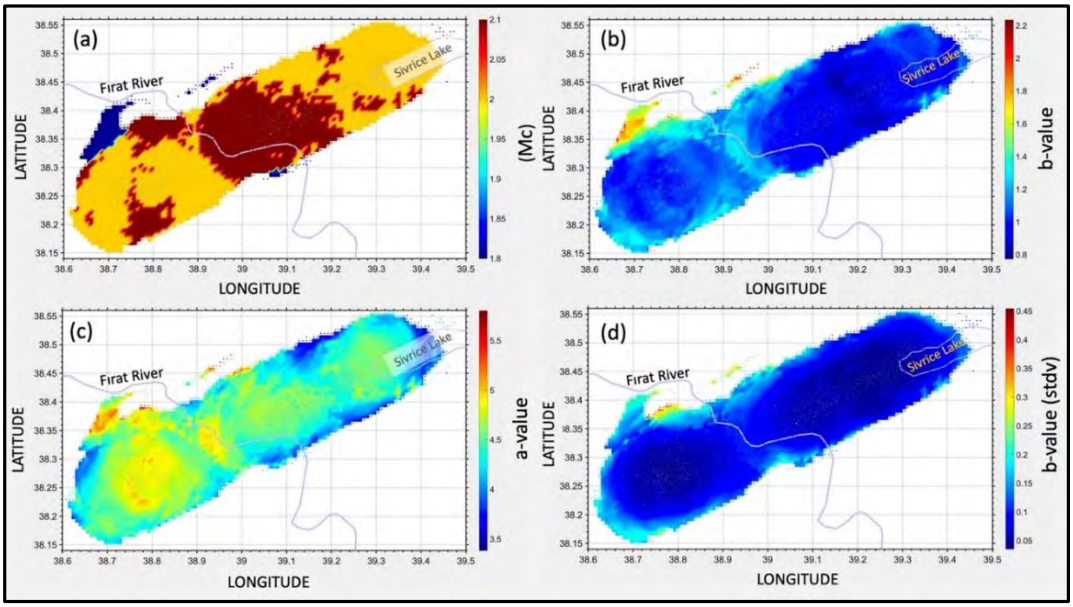


Figure 7. The spatial distribution of the G-R parameters of the 1.6≤Mw≤6.8 magnitude earthquake activity of the earthquake activity that occurred on the Pütürge Fault between January 1, 2018 and August 6, 2020. (a) Mc completeness magnitude, (b) b-value, (c) a-value and (d) the standard deviation of the b-value.

Şekil 7. 1 Ocak 2018 ile 6 Ağustos 2020 tarihleri arasında Pütürge Fayı'nda oluşan deprem etkinliğinin 1.6≤Mw≤6.8 büyüklüğündeki deprem aktivitesinin G-R parametrelerinin mekânsal dağılımı. (a) Mc tamlık büyüklüğü, (b) b-değeri, (c) a-değeri ve (d) b-değerinin standart sapması.

DISCUSSION AND CONCLUSION

In this study, seismological and seismotectonic properties of earthquake activity before and after the 24 January 2020 Mw6.8 earthquake on the Pütürge Fault, which did not cause strong earthquakes for a long time, were evaluated. The epicentral distributions of 5,482 earthquakes on the Pütürge Fault between January 1, 2018 and August 6, 2020 and the spatial and temporal changes of the Gutenberg-Richter parameters Mc, a- and b-values were examined. Before the mainshock on January 24, 2020, there were three earthquake clusters involving Mw≥4.0 earthquakes.These clusters started with the earthquakes on January 19, 2018 (Mw4.1), April 4, 2019 (Mw5.2) and December 27, 2019 (Mw4.9), respectively. The last two clusters occurred in the north and near (7 km) of the epicenter of the mainshock of January 24, 2020.

Focal mechanism solutions for earthquakes with magnitude Mw≥5.0, including the mainshock during the observation period, confirm the left-sided strike-slip fault mechanism compatible with field observations (Melgar et al., 2020; Kurcer et al., 2020). The northwest dipping fault planes obtained from focal mechanism solutions explain why the earthquake epicenters are concentrated in the northwest of the Pütürge Fault. Before the Sivrice-Doğanyol earthquake on January 24, 2020 (Mw6.8), an increase in Mc value was observed, while a significant decrease in b-value occurred and the decreasing trend continued for 28 days. It has been observed that the b-value decrease pattern is not significantly affected by the various grid spacing and sample window size applied in the data analysis and preserves the decreasing character. Since the 1970s, earthquake scientists have found convincing evidences in their research that the b-value decreased before many major earthquakes. Although discussions are still ongoing (Kamer and Hiemer, 2015), it can be said that these declining b-value anomalies give hope for long or mid-term prediction or forecasting the earthquakes. There are numerous observations in the laboratory that as the effective stress value applied to rock samples rise, the number of acoustic emissions emitted by micro-fractures increases and the b-value decreases significantly (Mogi, 1962; Main et al., 1989; Sammonds et al., 1992; Amitrano et al., 2005; Goebel et al., 2013; Scholz, 2015; Riviere et al., 2018; Lei et al., 2018).

Schorlemmer et al. (2005) suggested that the b-value is inversely related to the stress accumulated on the fault. Accordingly, an increase in stress will cause a decrease in b-value before the major break occurs, while the b-value will increase due to reduced stress after the earthquake. Gulia and Wiemer (2016, 2019) used examples of b-value decreasing patterns related to earthquakes for the 2016 Norcia (Italy) earthquake of magnitude 6.6 (Pino et al., 2019) and Kato et al. (2016) showed it for the 7.0 magnitude 2016 Kumamoto (Japan) earthquakes. Nuannin (2006), who conducted an eight-year observation at the Zinkruvan mine in Sweden, revealed that the pre-rockburst b-value displayed significant decreasing shapes.

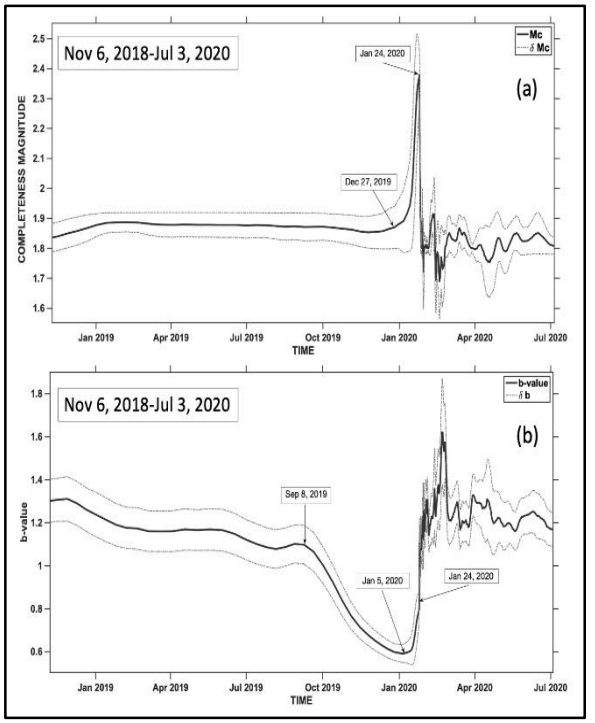


Figure 8. Temporal change of (a) Mc value and (b) b-value of the earthquake activity along the Pütürge Fault between Nov 6, 2018 and Jul 3, 2020. The arrows mark the beginning of change of the Mc and b-values and the origin time of mainshock of January 24, 2020 (Mw6.8). The dotted curve is the standard deviation values.
Şekil 8. Pütürge Fayı boyunca deprem aktivitesinin (a) Mc değeri ve (b) b-değerinin 6 Kasım 2018 ile 3 Temmuz 2020 arasında kaydedilen zamansal değişimi. Oklar, Mc ve b- değerleri ve ana şokun oluş zamanı 24 Ocak 2020 (Mw6.8) işaret etmektedir. Noktalı eğriler standart sapma değerleridir.

Studies conducted in various environments have shown that the b-value obeys the rule of inverse proportionality to effective stress in the tectonic environment (Wang,1988; Enescu and Ito, 2003; Helmstetter et al., 2003; Schorlemmer et al., 2005; Nanjo et al., 2012; Xie et al., 2019). It has been shown that the b-value of the earthquake storms that occurred between 1989-1997 before the Japan Tottori earthquake was 0.6 on average, and the b-value after the earthquake activity increased to 1.3-1.4 (Shibutani et al., 2002; Enescu and Ito, 2003). Wiemer and Wyss (2002) stated that b-value decreases where there is obstacle and asperity to the movements of faults.

It can be suggested that the reason for the decrease of the b-value before the main shock of 24 January 2020 (Mw6.8) is the increase in the effective stress on the Pütürge Fault and the preparation process of the fault for rupture. Based on the Mc value increase and b-value decrease anomalies obtained before January 24, 2020 (Mw6.8) mainshock of Sivrice-Doğanyol, it is recommended to monitor and evaluate the seismic activities on the major active faults of Turkey. In this context, the investigation of the earthquake hazard of the Erkenek Fault and the Pazarcık Fault (Duman and Emre, 2013), which have been silent in terms of strong earthquakes for decades and extend to the southwest of the Pütürge Fault, will be an important issue for earth scientists and seismologists. In the future, when earthquakes are monitored with more advanced seismic networks, the data quality that will provide spatial-temporal analysis of earthquake parameters is better, and new methods are developed, our hope for success in forecasting the earthquake hazard will increase.

ACKNOWLEDGMENTS

The earthquake data used in the article were obtained from Turkish Disaster and Emergency Management Authority (AFAD). I thank the editor in charge and Şerif Barış for their useful comments that improved an earlier version of the manuscript.

REFERENCES

AFAD (Disaster & Emergency Management Authority), 2020a. https://deprem.afad.gov.tr/ddakatalogu

AFAD (Disaster & Emergency Management Authority), 2020b. Report on 24 January 2020 Sivrice (Elazığ) Mw6.8 Earthquake, Disaster and Emergency Management Presidency of Turkey Ministry of Interior, Ankara, Turkey, (in Turkish), 46 pages.

Aki, K., 1965. Maximum likelihood estimate of b in the formula log(N)=a-bM and its confidence limits. Bull Earthq. Res. Int. Tokyo Univ., 43, 237-239.

Aktug, B, Ozener, H, Dogru, A, Sabuncu, A, Turgut, B, Halicioglu, K, Yilmaz, O, and Havazli, E., 2016. Slip rates and seismic potential on the East Anatolian Fault System using an improved GPS velocity field. J Geodynamics, 94-95: 1-12.

Allen, C. R., 1969. Active faulting in northern Turkey. Rep. 1577, Div. of Geol. Sic., Calif. Inst. of Technol., Pasadena, 32 pp.

Ambraseys, N.N., 1989. Temporary seismic quiescence: SE Turkey. Geophys. J. Int., 96, 311-331.

Ambraseys, N.N., and Jackson, J.A., 1998. Faulting associated with historical and recent earthquakes in the Eastern Mediterranean region. Geophys. J. Int. 133, 390–406.

Amitrano, D., Grasso J.R., and Senfaute, G., 2005. Seismic precursory patterns before a cliff collapse and critical point phenomena. Geophysical Research Letters, V. 32, Issue 8.

Arpat, E., and Saroglu, F., 1972. The East Anatolian Fault System: thoughts on its development. Bulletin of the Mineral Research and Exploration (MTA), 78: 33-39.

Arpat, E., and Saroglu, F., 1975. Some significant recent tectonic events in Turkey. Geological Society of Turkey Bulletin, 18, 91-101.

Bora, D.K., 2016. Scaling relations of moment magnitude, local magnitude, and duration magnitude for earthquakes originated in northeast India. Earthq. Sci., 29(3):153–164.

Brodsky, E.E., 2019. Predicting if the worst earthquake has passed. Nature, Vol 574, 185-186.

Dewey, J.F., Hempton, M.R., Kidd, W.S.F., Saroglu, F., and Sengor, A.M.C., 1986. Shortening of continental lithosphere: the neotectonics of Eastern Anatolia-a young collision zone. Collision Tectonics. London, UK: Geological Society of London Special Publications, Coward MP, Ries AC, (eds.), 3-36.

Dost, B., Edwards, B., and Bommer, J.J., 2018. The relationship between M and ML-a review and application to induced seismicity in the Groningen gas field, the Netherlands. Seismological Research Letters, 89(3), 1062-1074.

Duman, T.Y., and Emre, O., 2013. The East Anatolian Fault: geometry, segmentation and jog characteristics. Geological Society, London, Special Publications, 372, 495-529.

Emre, O., Duman, T.Y., Ozalp, S., Saroglu, F., Olgun, S., Elmaci, H., and Can, T., 2016. Active fault database of Turkey. Bulletin of Earthquake Engineering, V. 16, 3229–3275.

Enescu, B., and Ito, K., 2003. Values of b and p: their Variations and Relation to Physical Processes for Earthquakes in Japan. Annuals of Disas. Prev. Res. Inst., Kyoto Univ., No.46 B.

Eyidogan, H., and Hobbs, T.E., Recovery Underway Following Damaging 24 January 2020 Elazığ Earthquake in Eastern Turkey. Temblor, 2020. http://doi.org/10.32858/temblor.070

Goebel, T.H.W., Schorlemmer, D., Becker T.W., Dresen, G., and Sammis, C.G., 2013. Acoustic emissions document stress changes over many seismic cycles in stick-slip experiments. Geophysical Research Letters, V.40, Issue 10, 2049–2054.

Goertz-Allmann, B.P, Edwards, B., Bethmann, F., Deichmann, N., Clinton, J., Fah D., and Giardini, D., 2011, A New Empirical Magnitude Scaling Relation for Switzerland, Bulletin of the Seismological Society of America, 101 (6): 3088–3095.

Grünthal, G., Wahlström, R., and Stromeyer, D., 2009. The unified catalogue of earthquakes in central, northern, and northwestern Europe (CENEC). Journal of Seismology, V. 13, 613-632.

Gulia, L., and Wiemer, S., 2016. Short-term earthquake risk assessment considering time-dependent b-values. Geophysical Research Letters. 43(3).

Gulia L., and Wiemer S., 2019. Real-time discrimination of earthquake foreshocks and aftershocks. Nature, 574 (7777), 193-199.

Gutenberg, R., and Richter, C.F., 1944. Frequency of earthquakes in California. Bulletin of the Seismological Society of America, V. 34, 185–188.

Hainzl, S., 2016. Rate-Dependent incompleteness of earthquake catalogs. Seismological Research Letters, 87, 2A, 337-344.

Helmstetter, A., Sornette, D., and Grasso, J.R., 2003. Mainshocks are aftershocks of conditional foreshocks: How do foreshock statistical properties emerge from aftershock laws. Journal of Geophysical Research: Solid Earth, 108(B1).

Jackson, J., and McKenzie, D.P., 1984. Active tectonics of the Alpine-Himalayan belt between western Turkey and Pakistan. Geophys J Roy Astr S, 77: 185-264.

Kamer, Y., and Hiemer, S., 2015. Data-driven spatial b value estimation with applications to California seismicity: To b or not to b. J. Geophys. Res. Solid Earth, 120, 5191–5214.

Kato, A., Fukuda, J.I., Nakagawa, S., and Obara, K., 2016. Foreshock migration preceding the 2016 Mw7.0 Kumamoto earthquake, Japan. Geophysical Research Letters, 43 (17), 8945-8953.

Ketin, I., 1969. Türkiye'nin genel tektonik durumu ile başlıca deprem bölgeleri arasındaki ilişkiler. İ.T.Ü. Maden Fakültesi Dergisi, 130-135.

Kurcer, A., Elmaci, H., Yildirim, N., ve Ozalp, S., 2020. 24 Ocak 2020 Sivrice (Elazığ) Depremi (Mw=6,8) Saha Gözlemleri ve Değerlendirme Raporu, Maden Tetkik ve Arama Genel Müdürlüğü, Jeoloji Etütleri Dairesi, 7 Şubat 2020, Ankara. 41 sayfa.

Lei X., Wang, Z., and Su, J., 2018. The December 2018 ML5.7 and January 2019 ML5.3 earthquakes in South Sichuan Basin induced by shale gas hydraulic fracturing. Seismological Research Letters, 90(3).

Main, I., Meredith, P., and Jones, C., 1989. A reinterpretation of the precursory seismic b-value anomaly from fracture mechanics. Geophysical Journal, 96, 131-138.

MATLAB (2020), https://www.mathworks.com/products/new_products/release2018b.html

McKenzie, D. P., 1976. The East Anatolian fault: a major structure in eastern Turkey. Earth Planet Sc Lett., 29: 189-193.

McKenzie, D. P., 1978. Active tectonics of the Alpine-Himalayan belt: the Aegean Sea and surrounding regions. Geophysical Journal of the Royal Astronomical Society, 55, 217-254.

Melgar, D., Ganas, A., Taymaz, T., Valkaniotis, S., Crowell, B. W., Kapetanidis, V., Tsironi, V., Yolsal-Cevikbilen, S., and Ocalan, T., 2020. Rupture kinematics of January 24, 2020 Mw 6.7 Doganyol-Sivrice, Turkey earthquake on the East Anatolian Fault Zone imaged by space geodesy, Geophysical Journal International, V. 223, Issue 2, November 2020, 862–874.

Mogi, K., 1962. Magnitude-frequency relationship for elastic shocks accompanying fractures of various materials and some related problems in earthquakes. Bull. Earthquake Res. Inst. Univ. Tokyo, 40: 831-883.

Nanjo, K.Z., 2019. Were changes in stress state responsible for the 2019 Ridgecrest, California, earthquakes? Nature Communications, 10 pages.

Nanjo, K., Hirata, N., Obara, K., and Kasahara, K., 2012. Decade-scale decrease in b value prior to the M9-class 2011 Tohoku and 2004 Sumatra quakes. Geophys. Res. Lett., 39, L20304.

Nuannin, P., 2006. The potential of b-value variations as earthquake precursors for small and large events. Acta Universitatis Upsaliensis Uppsala, Digital Comprehensive Summaries of Uppsala Dissertations from the Faculty of Science and Technology, 183, 46 pp.

Pino, N. A., Convertito, V., and Madariaga, R., 2019. Clock advance and magnitude limitation through fault interaction: the case of the 2016 central Italy earthquake sequence. Scientific reports, 9(1), 5005.

Popandopoulos, G.A., Baskoutas, I., and Chatziioannou, E., 2016. The spatiotemporal analysis of the minimum magnitude of completeness Mc and the Gutenberg–Richter law b-value parameter using the earthquake catalog of Greece. Izvestiya, Physics of the Solid Earth, V. 52, 195–209.

Riviere, J., Lv, Z., Johnson, P.A., and Marone, C., 2018. Evolution of b-value during the seismic cycle: Insights from laboratory experiments on simulated faults. Earth and Planetary Science Letters, 482, 407–413.

Sammonds, P., Meredith, P., and Main, I.G., 1992. Role of pore fluids in generation of seismic precursors to shear fracture. Letters to Nature, Nature, V. 39, 228-230.

Scholz, C. H., 2015. On the stress dependence of the earthquake b value. Geophys. Res. Lett., 42, 1399–1402.

Schorlemmer, D., Wiemer, S., and Wyss, M., 2005. Variations in earthquake-size distribution across different stress regimes. Nature, 437, 539–542.

Sengor, A.M.C., 1987. Cross-faults and differential stretching of hanging walls in regions of low-angle normal faulting: examples from western Turkey. Geological Society, London, 575–589.

Shi, Y., and Bolt, B.A., 1982. The standard error of the magnitude-frequency b value. Bulletin of the Seismological Society of America, V. 72, No. 5, 1677-1687.

Shibutani, T., Nakao, S., Nishida, R., Takeuchi, F., Watanabe, K., and Umeda, Y., 2002. Swarm-like seismic activity in 1989, 1990 and 1997 preceding the 2000 Western Tottori Earthquake. Earth, Planets and Space, V. 54, 831–845.

Taymaz, T., Eyidogan, H., and Jackson, J., 1991. Source parameters of large earthquakes in the East Anatolian fault Zone (Turkey). Geophys. J. Int., 106, 537–550.

USGS,https://earthquake.usgs.gov/earthquakes/eventpage/us60007ewc/finite-fault.

Utsu, T., 1971. Aftershocks and earthquake statistics (iii)-analyses of the distribution of earthquakes in magnitude, time and space with special consideration to clustering characteristics of earthquake occurrence (1). Journal of the Faculty of Science, Hokkaido University, Ser. VII (Geophysics), 3, 379-441.

Wang, J., 1988. b-values of shallow earthquakes in Taiwan. Bulletin of the Seismological Society of America, 78 (3): 1243–1254.

Westaway, R., and Arger, J., 1996. The Gölbaşı basin, southeastern Turkey: a complex discontinuity in a major strike-slip fault zone. Geological Society, London,153, 729 – 743.

Wiemer, S., 2001. A software package to analyze seismicity: ZMAP. Seismological Research Letters, 72(3), 373-382.

Wiemer, S., and Wyss, M., 2002. Mapping spatial variability of the frequency-magnitude distribution of earthquakes. Advances in Geophysics, V. 45, 259-302.

Wu, Y.-M., Chen, S.K., Huang, T.-C., Huang, H.-H., Chao, and W.-A., Koulakov, I., 2018. Relationship between earthquake b-values and crustal stresses in a young orogenic belt. Geophysical Research Letters, 45, 1832–1837.

Xie, W., Hattori, K., and Ha, P., 2019. Temporal variation and statistical assessment of the b-value off the Pacific coast of Tokachi, Hokkaido, Japan. Entropy, 21, 249.